Estimation of Whole-Body Averaged SARs in Human Models for Far-Field Exposures in Whole-Body Resonance and GHz Frequency Regions

Akimasa Hirata [#1], Osamu Fujiwara[#2], Tomoaki Nagaoka[*3], and Soichi Watanabe [*4]
[#]*Nagoya Institute of Technology, Department of Computer Science and Engineering, Nagoya, Japan*
[*]*National Institute of Information and Communications Technology, Japan*
[1]ahirata@nitech.ac.jp, [2]fujiwara@odin.nitech.ac.jp, [3]nagaoka@nict.go.jp, [4]wata@nict.go.jp

***Abstract*— The purpose of the present study is to propose a scheme to estimate whole-body averaged specific absorption rate (WBA-SAR) in the whole-body resonance and GHz frequency regions. The motivation is that WBA-SARs in the child models in these frequency regions have been reported to approach to the basic restrictions in the international guidelines/standards. In the resonance frequency region, we proposed a formula to estimate WBA-SAR based on the antenna theory. The variability of WBA-SAR in the child models was given using the formula. The computational uncertainty in the WBA-SAR using the formula may be up to several percents especially due to the model inhomogeneity. The variability of the WBA-SAR due to model shape or Kaup index was found to be 30%. In the GHz region, we proposed a homogeneous ellipsoid having the electrical constants of muscle for a conservative WBA-SAR estimation. The applicability of that model was confirmed considering the infant model with different Kaup indexes. The variability of WBA-SAR with different Kaup indexes was shown to be 15%.**
***Key words*: whole-body averaged specific absorption rate (WBA-SAR), far field,**

I. Introduction

There has been increasing public concern about the adverse health effects of human exposure to electromagnetic (EM) waves. According to the safety guidelines of the ICNIRP (International Commission on Non-Ionizing Radiation Protection) [1] and the IEEE standard [2], the whole-body averaged specific-absorption-rate (WBA-SAR) is used as a metric of basic restriction for radio frequency (RF) whole-body exposures. The basic restriction of WBA-SAR is 0.4 W/kg for occupational exposure or 0.08 W/kg for public exposure. An incident electric /magnetic field, which does not produce EM absorption exceeding the above limit is defined as a reference level in the ICNIRP guidelines [1] and as the maximum permissible exposure in the IEEE standard [2]. The relationship between the reference level/maximum permissible exposure and the WBA-SAR was derived mainly from numerical calculations done dozens of years ago.

In computational dosimetry in the 1980s, human modeling was highly simplified in the figure of a prolate spheroid or a homogeneous block model [3, 4]. In recent years, with the development of computational resources, anatomically based human body models are used for investigating the WBA-SAR [5-11]. As the main result, the WBA-SAR under the reference level/ maximum permissible exposure is found to have a peak around several dozen megahertz due to standing waves over the body model. In addition, the WBA-SAR has another peak around 2 GHz, which is caused by a relaxation of the reference level/maximum permissible exposure with an increase in the frequency [6, 7, 9]. Furthermore, the WBA-SARs in the child models were larger than those in the adult [6, 7, 9, 10, 11].

The purpose of present study is to propsoe a scheme to estimate WBA-SAR in different human models for far-field exposure in these two frequency regions, in order to discuss the variability of WBA-SAR.

II. Computational Model and Methods

A. Computational Methods

The Finite-Difference Time-Domain (FDTD) method [12] is used for computational dosimetry. Either one of human models is located in free space. As a wave source, a plane wave with vertical polarization was considered. A 24-layered uniaxial-Perfectly Matched Layer was used as the absorbing boundary. The separation between the model and the absorbing boundary was set at 100 cells. The electrical constants of tissues were taken from a report by Gabriel [13].

B. Human Body Models

Whole-body voxel models for a Japanese adult male and a Japanese adult female were developed by Nagaoka et al. [14]. The resolution of these models was 2 mm segmented into 51 anatomical regions. Models for children of three, five and seven years of age were developed by applying a free form deformation algorithm to the male model. In this modeling, a total of 66 body dimensions was taken into account, and then reduced with different scaling factors. Manual editing was applied in order to maintain their anatomical validity. The resolution of these models was kept to 2 mm. More detailed explanation on these models can be found in [15].

For the discussion in the GHz region, we developed nine-month-old infant model. The reason for this is that Dimbylow and Bloch[10] reported that the WBSAR in a nine-month-old infant is larger than that in a three-year-old child model. For fundamental discussion on WBSAR, we considered

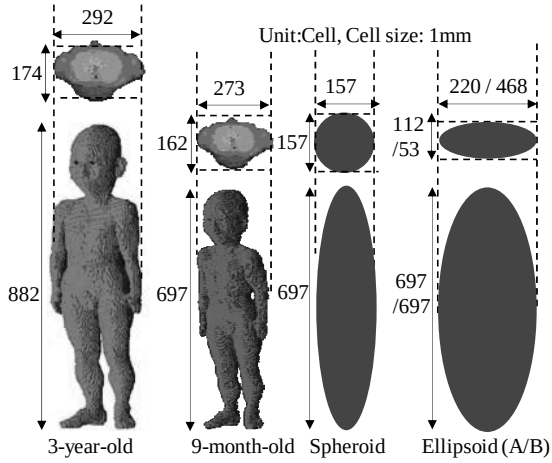

Fig. 1. Three-year-old child and nine-month-old infant models developed from three-year-old model. Spheroidal and ellipsoidal models correspond to the nine-month-old infant model.

Table 1. The parameters of the nine-month infant model and its corresponding simple-shaped models.

	Anthropomorphic	Spheroid	Ellipsoid	
			A	B
Height[m]	0.7	0.7	0.7	0.7
Weight[kg]	8.95	8.95	8.95	8.95
Eccentricity	-	0	0.86	0.99
S_M[m^2]	0.60	0.38	0.40	0.60
S_F[m^2]	0.12	0.09	0.12	0.26

S_M : Model surface area S_F : Frontally-projected area

spheroidal and ellipsoidal models corresponding to the above nine-month-old infant (see Fig. 1). The parameters of the spheroid were chosen so that its height and weight coincided with those of the infant model. We defined two ellipsoids (A and B) in terms of their eccentricity (circle: 0, parabola: 1), while their height and weight were identical to those of the infant model. The eccentricity of ellipsoid A was determined so that the frontally-projected area matched as that of the infant model, while that of ellipsoid B was determined based on the model surface area. The parameters of the models considered in the present studies are listed in Table 1.

III. Computational Results

A. *WBA-SAR Estimation in Whole-body Frequency Region*

The main purpose of this subsection is to propose an equation to estimate the WBA-SAR in order to discuss the variability of WBA-SAR in different human models. As shown in Section IIIA, as well as in previous studies [12-13], it is reasonable to consider the human body approximately as a half-wave dipole. The resonance frequency can be reasonably estimated from the height of the human subjects. The analogy of a half-wave dipole and human body models at their respective resonance frequency was confirmed in [18].

Let us summarize the fundamental characteristics of the half-wave dipole antenna. For the current distribution on the antenna $I(z)$ and the maximum current I_o [A], the effective height of the antenna L_e [m] is given by the following equation [17]:

$$L_e = \frac{1}{I_0}\int_0^L I(z)dz, \tag{1}$$

where L [m] is the physical height of the antenna. The effective height of the half-wave dipole is given by the following equation [17]:

$$L_e = \frac{\lambda}{\pi} \cong 0.636L. \tag{2}$$

For an antenna of known effective height, the induced voltage Vo [V] is given by multiplying the effective height by the incident electric field or incident power density S_{inc} [W/m^2]:

$$V_o = \sqrt{120\pi S_{inc}}\,L_e. \tag{3}$$

From (2) and (3), we can estimate the induced voltage in the antenna. We can obtain an equation to estimate the WBA-SAR in a human body model by the following equation:

$$\begin{aligned} WBSAR &\cong 7.52 S_{inc} H^2 / W \\ &= \quad 7.52 S_{inc} / B, \end{aligned} \tag{4}$$

where W is the weight of the human, and B ($=W/H^2$) [kg/m^2] is the body mass index (BMI). The coefficient has the dimension of m^2. Note that Conil et al. used BMI for discussing the variability in the WBA-SAR [9]. In that study, the WBA-SAR was not represented with the BMI. From Eq. (4), we can simply estimate the WBA-SAR in terms of BMI of the human body only.

In order to confirm the validity of the equation proposed, we show in Table 2 the comparison between FDTD-computed and estimated WBA-SAR in Japanese models. As seen from this table, the WBA-SARs estimated with (4) are in good agreement with those calculated with the FDTD method.

In terms of (4), we show in Fig. 2, the variability of WBA-SAR in different ages. Note that the BMI roughly follows the normal distribution [19]. The mean value and standard deviation σ for Japanese can be found in [20]. The BMI changes with the age of a human during childhood. It becomes minimal at five years of age. The mean value of BMI is 15.6 for a three-year-old child, 15.2 for a five-year-old child and 16.0 for a seven-year-old child. Their standard deviation is 1.3 for three-year-old and five-year-old children and 2.0 for a seven-year-old child. For the adult male, the mean value and standard deviation are 22.7 and 3.2, respectively. For the adult female, they are 21.3 and 3.1, respectively. Let us consider the WBSAR for the range of 2 σ, in order to cover over 95% of the Japanese population. From Fig. 1, the variability attributed to the BMI is also depicted in this figure. The higher and lower bounds in this figure correspond to the model with smaller and higher BMIs. The maximum WBSAR was observed in the five-year-old child because its BMI is the smallest. Note also that the variability of the WBSAR was found to be 30%, even for humans of the same age.

Table 2. Comparison of FDTD-Calculated and Estimated WBA-SARs ($\times 10^{-2}$ W/kg) in Japanese Male Models at Respective Resonance Frequencies (Power Density of 2 W/m^2)

	22 years	7 years	5 years	3 years
FDTD	7.03	9.38	9.34	9.11
Estimated	6.94	9.52	9.56	8.98
Diff. [%]	1.5	2.2	1.5	1.2

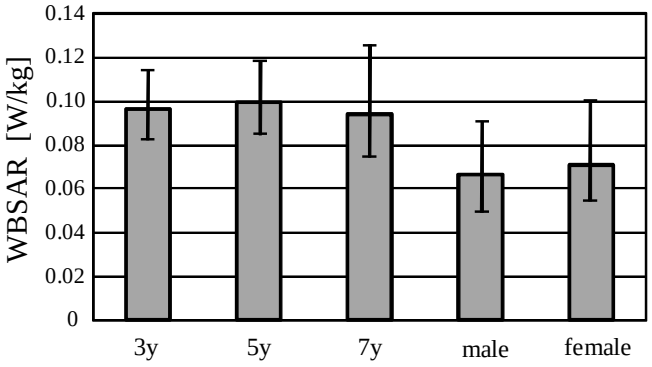

Fig. 2. Variability of WBSAR estimated with the proposed equation (2 W/m^2).

B. *Conservative Estimation of WBA-SAR in GHz Frequency Region*

In [11], we showed that the dominant factor influencing the WBA-SAR is the body surface area and electrical constants of tissues including the model inhomogeneity. In particular, due to the standing wave between tissue boundaries, it is difficult to evaluate the variability of WBA-SAR in different models. Due to the large expenditure of funds and the time involved, it is not realistic to develop many numeric human models of different heights and weights. In the standards/guidelines, homogeneous and simple-shaped models have been used in order to determine the reference level/maximum permissible exposure against the basic restriction of WBA-SAR. In these circumstances, the purpose of this section is to provide homogeneous and simple-shaped model which can yield overestimated WBA-SAR.

For this purpose, we considered nine-month child model and its corresponding spheroid and ellipsoids. The reason for choosing the nine-month child model is that in [10] the WBA-SAR in the nine-month child model has been reported to be larger than that in the child model. In addition, the computational cost considering the infant model is smaller than those for the children and adults.

The nine-month child model has been developed by linearly reducing the three-year child model given in Fig. 3. First, let us discuss the effect of model shape on the WBA-SAR. The WBA-SAR in the nine-month-old child model and its corresponding ellipsoidal/spheroidal models is plotted in Fig.3 for VP and HP.

In order to investigate the effect of model inhomogeneity, a homogeneous anthropomorphic model comprised of 2/3 muscle was also considered. As seen from Fig. 3, the spheroidal model and ellipsoidal model A gave an underestimation of WBA-SAR compared to the infant model over the frequency region considered, while the ellipsoidal model B gave an overestimation. For the ellipsoidal model B, the WBA-SARs for exposure with VP and HP are comparable, since the electromagnetic absorption in the GHz region is concentrated around the model surface. The feature of ellipsoidal model B is its small depth or large eccentricity, as shown in Table 1. The tendency in Fig. 3 was shown in the Japanese three-year-old child model, to which manual editing was conducted to keep the anatomical reliability.

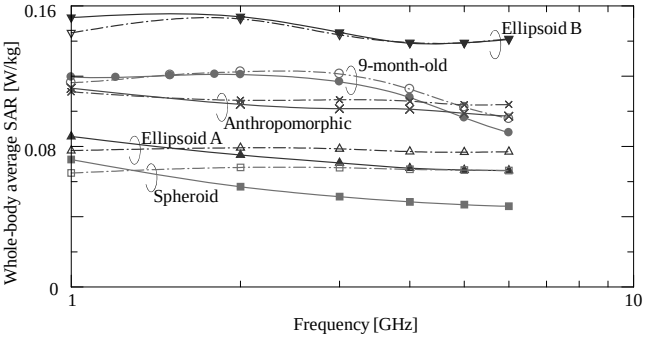

Fig. 3. Frequency characteristics of WBSARs for different body models (power density of incident wave was 10 W/m^2).

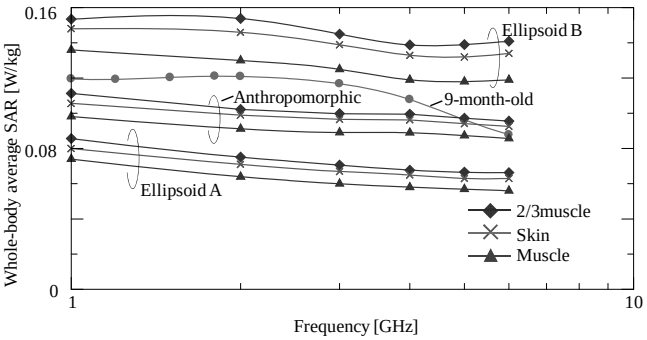

Fig. 4. Dependency of WBSAR on electrical constants of tissue for (a) VP and (b) HP (power density of incident wave was 10 W/m^2).

Fig. 4 shows the WBA-SAR in the models whose electrical constants are those of 2/3 muscle, skin, and muscle, which indicates the effect of electrical constants of the tissue on the WBA-SAR. From fig. 4, the WBA-SARs in the models with skin and muscle are 5% and 12-15% smaller, respectively, than that for 2/3 muscle, independent of the model shape. This tendency is identical to exposure with HP, although not shown here due to the lack of space, suggesting that the ellipsoid B whose electrical constants were chosen as those of muscle provides a conservative WBA-SAR. The same tendency was observed for the three-year-old child model, although it is not shown here for avoiding repetition.

Fig. 5 shows the frequency characteristics of the WBA-SAR for infant models with different Kaup indexes and their

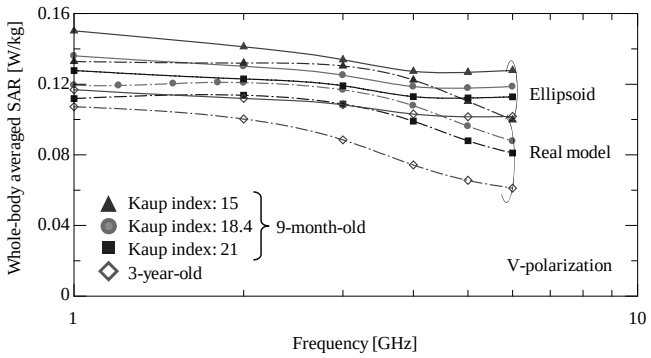

Fig. 5. WBSARs in nine-month-old infant and its corresponding conservative models with different Kaup indexes (power density of incident wave was 10 W/m^2).

conservative models proposed in the above subsection. Note that those for the three-year-old model is also plotted in order to confirm our idea. The Kaup index and BMI are essentially the same except for the unit and significant figures. The Kaup index is defined as the weight [g] divided by the square of the height [cm^2] multiplied by a factor of 10. The effectiveness of the conservative models proposed in the present study is confirmed from this figure, which also reveals that the variability of the WBA-SAR due to the model shape reaches ±15%. The WBA-SAR increased for infant models with a smaller Kaup index or lower weight. The effectiveness of the conservative model was confirmed for the three-year-old model whose anatomical construction is more reliable than those in the nine-month-infant models. Note that the same tendency was observed for HP, although the results were not shown here due to the lack of space.

IV. Conclusion

The WBA-SARs in the child models in the resonance frequency and GHz regions is of particular interest, since they are close to the basic restrictions in the international guidelines/standards. In the present study, we proposed a formula to estimate WBA-SAR in the whole-body resonance frequencies based on the antenna theory. The uncertainty in the WBA-SAR using the formula may be up to several percents especially due to the model inhomogeneity. The variability of WBA-SAR in the child models was given using the formula. In the GHz region, we proposed a homogeneous ellipsoid having the electrical constants of muscle as a conservative WBA-SAR estimation. The applicability of that model was confirmed considering the nine-month infant model with different Kaup indexes.

Acknowledgments

This work was supported in part by Grant-in-Aid for Scientific Research (B), and a Research Grant from Telecom Engineering Center, Japan.

References

[1] ICNIRP, "Guidelines for limiting exposure to time-varying electric, magnetic and electromagnetic fields (up to 300 GHz)," Health Phys. Vol.74, pp.494-522 (1998)

[2] IEEE Standard for Safety Levels with Respect to Human Exposure to Radio Frequency Electromagnetic Fields, 3 kHz to 300 GHz (C95.1), 2005.

[3] C. H. Durney, "Electromagnetic dosimetry for models of humans and animals: A review of theoretical and numerical techniques," *Proc. IEEE*, vol.68, pp.33-40, 1980.

[4] O. P. Gandhi, "State of the knowledge for electromagnetic absorbed dose in man and animals," *Proc. IEEE*, vol.68, pp.24-32, 1980.

[5] P. J. Dimbylow, "FDTD calculations of the whole-body averaged SAR in an anatomically realistic voxel model of the human body from 1 MHz to 1 GHz," *Phys. Med. Biol*., vol. 42, pp.479-490, 1997.

[6] P. J. Dimbylow, "Fine resolution calculations of SAR in the human body for frequencies up to 3 GHz," *Phys. Med. Biol.*, vol.47, pp.2835-2846, 2002.

[7] J. Wang, S. Kodera, O. Fujiwara, and S. Watanabe, "FDTD calculation of whole-body average SAR in adult and child models for frequencies from 30 MHz to 3 GHz," *Phys. Med. Biol.*, vol.51, pp.4119-4127, 2005.

[8] P. Dimbylow, "Resonance behavior of whole-body averaged specific absorption rate (SAR) in the female voxel model, NAOMI," *Phys. Med. Biol*., vol.50, pp.4053-4063, 2005.

[9] E. Conil, A. Hadjem, F. Lacroux, M. F. Wong, and J. Wiart, "Variability analysis of SAR from 20 MHz to 2.4 GHz for different adult and child models using finite-difference time-domain", *Phys. Med. Biol*., vol.53, pp.1511-1525, 2008.

[10] P. Dimbylow and W. Bolch, "Whole-body-averaged SAR from 50 MHz to 4 GHz in the University of Florida child voxel phantoms," *Phys. Med. Biol.*, vol. 52, pp.6639-6649, 2007.

[11] A. Hirata, S. Kodera, J. Wang, and O. Fujiwara, "Dominant factors for influencing whole-body average SAR due to far-field exposure in whole-body resonance frequency and GHz regions," *Bioelectromagnet*, vol.28, pp.484-487, 2007,"

[12] A. Taflove and S. Hagness, *Computational Electrodynamics: The Finite-Difference Time-Domain Method* 3rd edn (Norwood, MA: Artech House Publishers), 2003

[13] C. Gabriel C, Compilation of the dielectric properties of body tissues at RF and microwave frequencies. *Brooks Air Force Technical Report* AL/OE-TR-1996 -0037, 1996.

[14] T. Nagaoka, S. Watanabe, K. Sakurai, E. Kunieda, S. Watanabe, M. Taki, and Y. Yamanaka, "Development of realistic high-resolution whole-body voxel models of Japanese adult males and females of average height and weight, and application of models to radio-frequency electromagnetic-field dosimetry," *Phys. Med. Biol*., vol.49, pp.1-15, 2004.

[15] T. Nagaoka, E. Kunieda, and S. Watanabe, "Proportion-corrected scaled voxel models for Japanese children and their application to the numerical dosimetry of specific absorption rate for frequencies from 30 MHz to 3 GHz," *Phys. Med. Biol*., vol.49, pp.1-15, 2004.

[16] D. Poljak, C. Y. Tham, O. Gandhi, and A. Sarolic, "Human equivalent antenna model for transient electromagnetic radiation exposure," *IEEE Trans. Electromagnetic Compat.* Vol.45, no.1, pp.141-145, 2003.

[17] J. D. Kraus and R. J. Marhefka, Antennas for all applications, 3rd Ed. McGraw-Hill, NY, 2002.

[18] O. P. Gandhi and E. Aslan, "Human equivalent antenna for electromagnetic fields," US Patent no.5394164, Feb. 28, 1995.

[19] A. D. Penman and W. D. Johnson, "The changing shape of the body mass index distribution curve in the population: implications for public health policy to reduce the prevalence of adult obesity," *Prev. Chronic Dis.*, vol.3, no.3, A74.

[20] S. Komiyama, T. Masuda, T. Nakao, and K. Teramoto, "The relationships between stature, fat-free mass index, and fat mass index at before and after BMI-rebound in children," *J. Health Sci.*, vol.26, pp.31-39, 2004.